Published in final edited form as:
J Neurochem. 2011 July ; 118(2): 215–223. doi:10.1111/j.1471-4159.2011.07319.x.

Mouse MCP1 C-terminus inhibits human MCP1-induced chemotaxis and BBB compromise

Yao Yao and **Stella E. Tsirka**
Program in Molecular and Cellular Pharmacology, Dept of Pharmacological Sciences, Stony Brook University, Stony Brook, NY 11794-8651

Abstract

Compared to the rodent monocyte chemoattractant ptotein 1 (MCP1/CCL2), the human MCP1 lacks a C-terminal extension. Although the function of this C-extension is not entirely defined, in previous work we reported that it decreases the chemotactic properties of mouse MCP1. To determine if this function is specific to the rodent chemokine, or if the C-terminal extension has the ability to regulate chemotactic potency to MCP1 in general, we generated a chimeric protein consisting of human MCP1 fused to the mouse MCP1 C-terminal fragment. We found that mouse MCP1 C-terminus significantly decreased the chemotactic potency of human MCP1 and diminished the BBB compromise normally induced by the human protein. Not only did mouse MCP1 C-terminus inhibit human MCP1-induced Rac1 activation and formation of lamellipodia, it also disrupted the staining pattern of ZO-1 at cell-cell borders and prevented human MCP1-induced F-actin formation in brain microvascular endothelial cells. Additionally, the MCP1 C-terminus dramatically decreased human MCP1-induced activation of ERM proteins in endothelial cells. These findings confirm that the rodent C-terminal MCP1 extension acts as a rheostat for MCP1 functions and suggest that potentially in humans another protein or protein complex may assume a similar regulatory function.

Introduction

When a brain injury occurs, microglia, the brain resident immune cells, become activated and migrate to the site of injury. The integrity of blood brain barrier (BBB) becomes compromised and peripheral blood cells infiltrate across the disrupted BBB into the brain parenchyma. The activated microglia together with the infiltrated immune cells can affect the outcome of the injury. Monocyte chemoattractant protein-1 (MCP1, also known as CCL2), a chemokine transiently but dramatically over-expressed during brain injury, is involved in the chemotaxis of microglia/monocytes (Sheehan et al., 2007, Yao and Tsirka, 2010) and compromise of BBB (Stamatovic et al., 2003, Stamatovic et al., 2005, Dimitrijevic et al., 2006, Stamatovic et al., 2006; Yao and Tsirka, 2011).

MCP1 is conserved among species in the N-terminus but not in the C-terminus. Mouse MCP1 has 148 amino acids, whereas the human MCP1 only has 99 amino acids. Previous studies in our lab have shown that plasmin cleaves mouse MCP1 at lysine 104 (K104), generating an N-terminal fragment highly homologous to human MCP1 and a C-terminal extension (Sheehan et al., 2007). Our previous studies revealed that the mouse MCP1 lacking the C-terminus (K104Stop-MCP1) has a much higher chemotactic potency than the full length one (FL-MCP1) (Sheehan et al., 2007, Yao and Tsirka, 2010). Although the C-

Address correspondence to: Stella Tsirka, Dept Pharmacology, BST8-192, SBU, Stony Brook, NY 11794-8651; Tel: 631-4443859, Fax: 631-4443218, stella@pharm.stonybrook.edu.

The authors declare that they have no conflicts of interest.

terminal extension promotes oligomerization of MCP1, it decreases the affinity between MCP1 and its receptor CCR2, inhibits the activation of Rac1 and formation of lamellipodia in microglia (Yao and Tsirka, 2010). In addition, the plasmin-truncated MCP1 disrupted more effectively the integrity of BBB (Yao and Tsirka, 2011). The redistribution of occludin and ZO-1 and reorganization of actin cytoskeleton as well as phosphorylation of ERM proteins are responsible for the compromise of BBB integrity (Stamatovic et al., 2003, Stamatovic et al., 2006; Yao and Tsirka, 2011). These data suggest that mouse MCP1 is regulated via auto-inhibition by its C-terminus.

In this study we assessed whether the mouse C-terminal extension can exert a regulatory function on human MCP1 by evaluating the functions of a chimeric protein carrying the human N-terminus fused to the mouse C-terminal extension. Our results indicate that such function is indeed mediated by the mouse C-terminal extension, raising the possibility that in the human system another protein or protein complex functions to inhibit a constitutive activity of MCP1.

Methods

Animals

C57BL/6 (wild-type) and MCP1$^{-/-}$ mice were purchased from the Jackson Laboratories. These mice were maintained and bred in the Department of Laboratory Animal Research at Stony Brook University with free access to water and food ad libitum. MCP1$^{-/-}$ mice have already been backcrossed for 12 generations to the C57BL/6 background. All experimental procedures were performed using mice from both genders in accordance to the National Institutes of Health guide for the care and use of laboratory animals and the institutional guidelines established by the Institutional Animal Care and Use Committee at Stony Brook University (Assurance A3011-01 and protocol 2011-0676).

Cell Culture

N9 cells (originally provided by Dr. S. Barger at University of Arkansas, Fayetteville and Dr. P. Ricciardi-Castagnoli at University of Milano-Bicocca, Milan) were maintained in Modified Eagle's Medium (MEM) supplemented with 10% fetal bovine serum (FBS), 100 U/ml penicillin and 100 μg/ml streptomycin at 37°C with 5% CO2. CHME3 cells (a human microglial cell line kindly provided by Dr. M. Naghavi, Columbia University, New York) were cultured as described (Haedicke et al., 2009).

Mouse brain microvascular endothelial cells (BMEC, CRL2299) and mouse astrocytes (CRL2541) were purchased from ATCC and cultured in Dulbecco's Modified Eagle's Medium (DMEM) supplemented with 10% FBS, 100 U/ml penicillin and 100 μg/ml streptomycin at 37°C with 5% CO2.

Primary microglia were collected from mixed cortical cultures as described previously (Giulian and Baker, 1986, Yao and Tsirka, 2010). Briefly, brains from 1-day-old pups were collected. The meninges and hippocampi were removed and the cortical tissue was digested with trypsin (0.25% in Hanks balanced saline solution, HBSS) for 15 minutes at 37°C. Then the cortices were mechanically dissociated by trituration followed by filtration through a 70μm cell strainer. The filtered cell suspensions were plated onto culture dishes coated with poly-D-lysine and maintained in DMEM supplemented with 10% FBS. The medium was changed on day 3. On day 14, microglia were collected by addition of 15mM lidocaine for 10 minutes at room temperature followed by centrifugation. The microglia were used immediately (migration assays) or maintained in DMEM with 1% FBS for 2 days (for other experiments).

Primary mouse BMEC were isolated and cultured as described previously (Deli et al., 2003, Calabria et al., 2006; Yao and Tsirka, 2011). Briefly, brains from 3–5-week-old mice were collected and cut into hemispheres. The hemispheres were rolled on sterile Whatman chromatography paper to remove the meninges. The cortices were minced, triturated, and digested with collagenase (0.7 mg/ml) and DNase I (39 U/ml) at 37°C for 1 h. Then the solution was diluted with DMEM and centrifuged at 1000 g for 8 min at 4°C. The pellet was re-suspended in 20% bovine serum albumin and centrifuged at 1000 g for 20 min at 4°C. The microvessel rich pellet was digested with collagenase/dispase (1 mg/ml), DNase I (39 U/ml) at 37°C for 1 h, then diluted with DMEM and centrifuged at 700g at 4°C for 7 min. The pellet was re-suspended and layered over a 33% continuous Percoll gradient and centrifuged at 1000g for 10 min at 4°C. The microvessel layer was collected using an 18-gauge needle and diluted with DMEM. After centrifuging at 700g for 10 min at 4°C, the pellet was maintained in complete culture medium (DMEM supplemented with 20% bovine pletelet-poor plasma-derived serum (Biomedical Technologies Inc.), 100 μg/ml heparin, 1 ng/ml basic fibroblast growth factor, 4μg/ml puromycin, 100 U/ml penicillin and 100 μg/ml streptomycin) and plated on type IV collagen (400 μg/ml) and fibronectin (100 μg/ml) pre-coated plates or coverslips. The culture medium was changed every 24 h after initial plating. From day 3, complete culture medium without puromycin was used.

Generation of 6xHis-tagged MCP1 proteins

Human-MCP1 (h-MCP1) and human MCP1 with C-terminal extension of mouse MCP1 (hc-MCP1) were subcloned without the signal peptide into pET vectors with an N-terminal 6xHis tag. The constructs were transformed into BL21 cells and expression of the target proteins was induced using isopropyl-beta-D-thiogalactopyranoside for 5 hours. Recombinant proteins were purified utilizing a cobalt affinity resin (Clontech, Cambridge, UK). The collected fractions were analyzed on 16% Tris-Tricine sodium dodecyl sulfate polyacrylamide gel electrophoresis (SDS-PAGE) by coomassie blue staining. The purified proteins were confirmed by immunoblotting using 1:1000 anti-MCP1 antibodies (Serotec and Cell Sciences) or 1:1000 anti-6xHis antibody (Santa Cruz Biotechnology).

Western Blot Analysis and Immunoblotting

RIPA buffer (50mM Tris-HCl pH 7.4, 150mM NaCl, 1% NP40, 0.25% sodium deoxycholate, 1mM PMSF, 1x protease inhibitor cocktail, 1x Na3VO4) was used to lyse cells. Lysates containing equal amounts of proteins were resolved in 10% or 15% SDS-PAGE and transferred to Immobilon-P transfer membranes (Millipore). The target proteins were visualized using 1:1000 anti-CCR2, 1:1000 anti-tubulin, 1:1000 anti-Rac1, 1:1000 anti-pERM, 1:1000 anti-pERK, 1:1000 anti-ERK antibodies.

Competitive Binding Assay

The competitive binding assay was performed as previously described (Biber et al, 2003) with minor modifications: CHME3 cells were plated in 96-well plate and incubated with LPS (100ng/ml) for 12 hours. Then, the cells were incubated with 50nM biotinylated human MCP1 (R&D Fluorokine) with or without increasing concentrations of unlabeled h- or hc-MCP1 for 1 hour at 4°C. This was followed by a 30-minute incubation with FITC-Avidin at 4°C. After extensive wash, the cell-surface FITC signal was captured and quantified by a plate reader (Fluoroskan Ascent, Thermo Electron Corporation). The FITC signaling was then normalized to total protein concentration and expressed as percentage of fluorescence in the absence of unlabeled MCP1.

Rac Activition Assay

Activated Rac was pulled down as previously described (Yao and Tsirka, 2010). GST-PBD immobilized to glutathione beads was generously provided by Dr. J. Prives at Stony Brook University. Microglia were treated with 10nM MCP1 proteins for varied times. The activated Rac was pulled down using the GST-PBD beads and detected by immunoblotting. Total Rac1 was determined by immunoblotting the cell lysates. Fluorescence intensities were quantified using Odyssey Infrared Imaging software. Rac activation in stimulated cells was normalized to the amount of activated Rac in control microglia.

Membrane Sheet Assay

This assay was performed as previously described (Yao and Tsirka, 2010). Briefly, primary microglia were seeded on coverslips and activated with 100ng/ml LPS overnight. Then the cells were stimulated with 10nM h- or hc-MCP1 for 1 hour at 37°C, followed by swelling in hypotonic buffer (25mM KCl, 10mM Hepes, 2mM MgCl2, 1mM EGTA, 1mM PMSF, 1x protease inhibitor cocktail, pH 7.5) for 20 minutes. Next, the cells were washed, fixed with 4% paraformaldehyde, permeabilized and stained with 1:1000 rat-anti-Mac2 antibody (BD Pharmingen) and 1:500 rabbit anti-CCR2 antibody (Epitomics). The cells were visualized by 1:1000 fluorescence-conjugated secondary antibodies (Invitrogen) and imaged using Zeiss LSM510 confocal microscopy.

Immunofluorescent imaging of the F-actin cytoskeleton

To mimic endogenous chemoattractant gradient, a point source of MCP1 was created as previously described (Yao and Tsirka, 2010). In brief, heparin was spotted at the edge of 12-well plates. 15μl of h- or hc-MCP1 was then added directly onto the dried heparin spot. After 1h, primary microglia attached to coverslips were placed in the well. At each time point, the cells were washed and fixed with 4% paraformaldehyde. After washing, the cells were incubated with 1:500 Alexa-488 phalloidin overnight at room temperature, washed, mounted using FluorMount with DAPI, and imaged using confocal microscopy.

Migration Assay

Migration assays were performed using chemotactic chambers (Boyden; NeuroProbe) as described previously (Yao and Tsirka, 2010). Recombinant h- or hc-MCP1 was suspended in MEM with or without the Rac inhibitor, NSC23766 and added to the bottom chamber. Microglia suspended in MEM (2 × 105/ml) with or without the Rac inhibitor were added to the upper chamber, with a 5.0μm filter inserted between the chemoattractants and microglial cells. Migration was allowed to proceed for 2.5 h at 37°C. After wiping off cells that failed to migrate, the cells that migrated into or through the membrane were fixed and stained with hematoxylin. The membranes were photographed at 100X magnification. Total migration was quantified by counting stained cells. The background for random cell movement (cells responding to MEM only) was subtracted.

Transendothelial Electrical Resistance (TEER) Assay

The BMEC-astrocyte co-culture system was constructed as described (Stamatovic et al., 2005, Dimitrijevic et al., 2006; Yao and Tsirka, 2011). In brief, astrocytes were seeded on the lower side of the 0.4 μm Transwell inserts. After 4 h, the inserts were inverted and BMEC were plated in the upper chamber. 5 days later, 100 nM h-, and hc-MCP1 were added to the lower chambers. At each time point, TEER values were measured using the EVOM Epithelial Volt-ohm-meter (World Precision Instruments). The resistance of empty inserts were also measured and subtracted for calculation of final TEER values ($\Omega \cdot cm^2$).

In vitro Permeability Assay

The leakage of BBB was assessed in vitro as described previously (Stamatovic et al., 2003, Stamatovic et al., 2005, 2006; Yao and Tsirka, 2011). Briefly, the co-culture system or the primary BMEC monolayer was prepared as described above. Sterile FITC-Dextran (Mw 3000–5000 Dalton) was added into the upper chamber and 100nM h-, and hc-MCP1 were added to the lower chambers. At each time point, 100μl sample from the lower chamber was withdrew and 100μl fresh medium with 100 nM MCP1 was added back to the lower chamber. The amount of dextran in the lower chamber was quantified by reading the collected samples at 480nm. The OD values were converted to the concentration of FITC-Dextran in the lower chamber based on a standard curve.

Immunofluorescent Staining

Primary BMEC were plated on coverslips and treated with 100 nM h- or hc-MCP1 for 2 hours. After fixed in 4% formaldehyde for 20min, the cells were incubated with 1:300 rabbit anti-ZO-1 antibody (ZYMED) followed by 1:1000 fluorescent secondary antibodies (Invitrogen). For phalloidin staining, the cells were fixed with 4% formaldehyde and stained with 1:1000 Alexa-488 phalloidin overnight at 4°C. The staining was examined using Zeiss LSM510 confocal microscopy.

Triton X-100 fractionation

Triton X-100 fractionation was performed as described previously with minor modifications (Stamatovic et al., 2006; Stamatovic et al., 2003; Stamatovic et al., 2005; Yao and Tsirka, 2011). Briefly, extracting buffer (10 mM Tris-HCl pH 7.4, 100mM NaCl, 300 mM sucrose, 0.5% Triton X-100 and protease inhibitor cocktail) was added on top of a confluent monolayer of BMECs. Extraction was performed by gently rocking at 4°C for 20 minutes. Collected supernatants were defined as the Triton-X-100-soluble fraction. The cell pellet, which still adheres to the culture dishes, was washed twice with PBS supplemented with protease inhibitor cocktail and lysed with radioimmunoprecipitation assay buffer (RIPA buffer: 10 mM Tris-HCl pH 7.4, 140 mM NaCl, 1% sodium deoxycholate, 0.1% SDS, 1% Triton X-100 and protease inhibitor cocktail). Collected supernatants were defined as the Triton-X-100-insoluble fraction. Both Triton-X-100-soluble and -insoluble fractions were prepared by adding 4X SDS sample loading buffer and heating at 95°C for 10 minutes.

Statistics

Results are shown as Mean ± SD. The Student's t-test was used to analyze difference between two groups. *$p<0.05$ was considered significant.

Results

Plasmin cleaves off the mouse MCP1 C-terminus from the chimeric MCP1 protein

A recombinant human MCP1 (h-MCP1) and a chimeric protein consisting of the human MCP1 sequence fused with the C-terminal extension of the mouse MCP1 (hc-MCP1) were generated. To test whether these MCP1 proteins can be cleaved by plasmin, they were incubated with the protease for 2h at 37°C. Treatment of hc-MCP1 with plasmin led to degradation of the 18kD intact protein and detection of a 13kD fragment corresponding to h-MCP1. h-MCP1 remained intact despite the treatment with plasmin (Supplemental Figure 1).

The mouse MCP1 C-terminus interferes with the interaction between human MCP1 and CCR2

We have previously reported that the C-terminus of mouse MCP1 affects the interaction of the rodent chemokine with its receptor CCR2 (Yao and Tsirka, 2010). Similarly we explored whether the C-terminus of mouse MCP1 could also affect the interaction of human MCP1 with CCR2. We assessed the chemokine effect on the total cellular level of CCR2 expressed by microglial cells. Our data showed that although h-MCP1 or hc-MCP1 treatment did not affect the total cellular CCR2 levels (Supplemental Figure 2), both recombinant proteins decreased membrane bound CCR2 (using a membrane sheet assay); however the effect of h-MCP1 was much more potent than that of hc-MCP1 (Figure 1), suggesting that the C-terminus of mouse MCP1 interferes with the h-MCP1-CCR2 interaction. This is consistent with the effect of the C-terminus on the affinity between mouse MCP1 and CCR2 (Yao and Tsirka, 2010).

To further examine the affinity of these recombinant MCP1 proteins for CCR2, we performed a competitive binding assay, as previously described (Biber et al., 2003). We found a significant decrease of FITC signaling in the presence of increasing concentration of h-MCP1 (Figure 1B), suggesting replacement of biotinylated MCP1 by unlabeled h-MCP1. On the contrary, hc-MCP1, was not able to replace the bound biotinylated MCP1 even at 25μM (500X) (Figure 1B). These data reveal that h-MCP1 has a much higher affinity for CCR2 than hc-MCP1.

The mouse MCP1 C-terminal extension decreases the chemotactic potency of human MCP1

To test whether addition of the C-terminus to human MCP1 affects the chemokine's potency, we performed Boyden chamber migration assays using recombinant h- and hc-MCP1. As shown in Figure 2A, h-MCP1 elicited a strong chemotactic response (584±101 cells), whereas hc-MCP1 had only a moderate response (98±41 cells), indicating that the C-terminal tail inhibits the chemotaxis initiated by human MCP1. A similar trend was obtained when the human microglial cell line CHME3 was used to assess the chemotactic potency of the two recombinant proteins (Figure 2A right panel).

In the presence of NSC23766, a Rac1 specific inhibitor, on the other hand, neither h- or hc-MCP1 was able to induce the migration of microglia (Figure 2A left), thus confirming that Rac is a key player in MCP1-induced migration. The effect of h-MCP1 vs hc-MCP1 on activated Rac was directly assessed using a Rac activation assay. h-MCP1 treatment led to a transient but dramatic activation of Rac (Rac-GTP), whereas hc-MCP1 was slower in activating Rac, and that only to low levels (Figure 2B). This piece of data is consistent with our previous data that mouse MCP1 lacking the C-terminus is able to activate Rac whereas intact mouse MCP1 fails to activate Rac (Yao and Tsirka, 2010). When the activation assay was repeated with the human microglia (Figure 2C), once again h-MCP1 activated Rac dramatically, although the activation rate appeared to be slower.

Mouse MCP1 C-terminal extension prevents the formation of lamellipodia

The next step in the migration process following activation of Rac is the formation of lamellipodia (Maghazachi, 2000, Pankov et al., 2005, Terashima et al., 2005). Since mouse MCP1 C-terminus affects human MCP1-induced microglial migration and Rac activation, we further investigated its effect on the formation of lamellipodia. Using the method we described before (Yao and Tsirka, 2010), we created a point source of h- and hc-MCP1 and quantified the percentage of unipolar cells (the cells that are able to migrate). Our data showed that h-MCP1 was able to increase the number of unipolar cells since 15 minutes after treatment and up to 2 hours (Figure 3A). This effect diminished over time, although it

was still significantly higher than Ctr at 2h time point (Figure 3A). It should be noted that this pattern is similar to that of commercial human MCP1 (without 6His tag) (Yao and Tsirka, 2010), suggesting that our recombinant MCP1 proteins are biologically active. Unlike h-MCP1, the effect of hc-MCP1 did not decay over time (Figure 3A). Although hc-MCP1 had a much lower effect than h-MCP1 at 15-minute time point, no difference was found at other time points (Figure 3A). Similar to h-MCP1, hc-MCP1 significantly enhanced the number of unipolar cells, compared with ctr (Figure 3A). The effect of hc-MCP1 is comparable to that of mouse full length-MCP1 (approximately 20% of unipolar cells) (Yao and Tsirka, 2010), suggesting that the C-terminus of mouse MCP1 affects human MCP1 in the same manner as it does in mouse system. These data suggest that human MCP1 may be regulated in the same way as mouse MCP1---by an unknown protein or protein complex functioning just like the C-terminus of mouse MCP1. We tried to pull down the protein or protein complex using anti-human MCP1 antibody or anti-6His antibody via immunoprecipitation, but it did not work, probably due to the sensitivity of the immunoprecipitation method.

Mouse MCP1 C-terminus promotes a delayed but dramatic activation of ERK

Previous studies in our lab have shown that the C-terminal extension affects mouse MCP1-induced activation of MAPK pathway in microglial cells (Yao and Tsirka, 2010). Thus, we further studied whether it was the same case for human MCP1. Similar to K014Stop-MCP1, h-MCP1 promoted an early but fast activation of ERK (Figure 3B). Like mouse FL-MCP1, hc-MCP1 induced a prolonged activation of ERK (starting at 30 minutes and up to 2 hours) (Figure 3B). Surprisingly, the effect of hc-MCP1 was much higher than that of h-MCP1 or FL-MCP1 (Yao and Tsirka, 2010), suggesting hc-MCP1 and FL-MCP1 have different functions.

Mouse MCP1 C-terminus abrogates the BBB-disrupting activity of human MCP1

In addition to the chemotactic activity, we also investigated the activity of these recombinant MCP1 proteins to compromise BBB integrity. We used an in vitro BBB model by co-culturing BMEC and astrocytes as described previously (Yao and Tsirka, 2011). Since BMEC have endogenous plasmin activity and plasmin cleaves the C-terminus off from the chimeric protein, α2-antiplasmin, a specific plasmin inhibitor, is used in our co-culture system to block the endogenous plasmin activity. Our data showed that h-MCP1 significantly lowered the TEER value (Figure 4A), indicating a disruption of BBB integrity. hc-MCP1, however, failed to decrease the TEER (Figure 4A). We also performed the TEER assay on primary BMEC monolayer with comparable results (Figure 4A right panel, primary BMECs): h-MCP1 significantly lowered the TEER, indicating compromise of BBB, whereas hc-MCP1 was unable to do so. Consistent with the TEER data, h-MCP1 dramatically enhanced the permeability of FITC-Dextran across the co-culture system, whereas hc-MCP1 failed to do so (Figure 4B). These data suggest that the C-terminus of mouse MCP1 is inhibitory to MCP1-induce BBB disruption in human system.

Mouse MCP1 C-terminus prevents the redistribution of ZO-1 and reorganization of actin cytoskeleton induced by human MCP1

It has been reported that mouse MCP1 promotes the compromise of BBB through activation of ERM proteins, which bind to ZO-1 and actin cytoskeleton, and reorganization of actin cytoskeleton, which pulls tight junction proteins away from cell-cell border (Yao and Tsirka, 2011). Here we showed that h-MCP1 induced disruption of ZO-1 staining at the cell-cell border of primary BMEC, whereas hc-MCP1 did not changed the staining pattern of ZO-1 (Figure 4C upper panels). It has been shown that MCP1 treatment promotes the association of tight junction proteins with actin cytoskeleton (Stamatovic, et al, 2003, 2005, 2006). We thus extracted Triton X-100 soluble (contains free tight junction proteins) and insoluble

(includes actin associated tight junction proteins) fractions and performed semiquantitative western blot for ZO-1 and occludin. In agreement with previous reports (Stamatovic et al., 2006; Stamatovic et al., 2003; Stamatovic et al., 2005; Tsukamoto and Nigam, 1997; Tsukamoto and Nigam, 1999), h-MCP1 specifically induced the shift of ZO-1 and occludin from Triton X-100 soluble fraction to insoluble fraction, suggesting increased interaction between tight junction proteins and actin cytoskeleton. hc-MCP1, on the other hand, did not change the distribution of tight junction proteins (Supplemental Figure 3). Consistently, h-MCP1 significantly increased the F-actin in primary BMEC, suggesting reorganization of actin cytoskeleton (Figure 4C lower panels). hc-MCP1, on the contrary, had no or little effect on F-actin (Figure 4C lower panels). The effect of h- and hc-MCP1 was similar to that of K104Stop-MCP1 and K104A-MCP1 (plasmin non-cleavable mouse MCP1), respectively (Yao and Tsirka, 2011), again suggesting that the C-terminus of mouse MCP1 is inhibitory to human MCP1.

Mouse MCP1 C-terminus inhibits the human MCP1-induced phosphorylation of ERM proteins

Phosphorylation of ERM proteins contributes to the redistribution of tight junction proteins induced by mouse MCP1. Previous studies in our lab showed that in the mouse system FL-MCP1 and K104Stop-MCP1 significantly promoted the phosphorylation of ERM proteins, whereas full length MCP1 failed to do so in the presence of A2AP (Yao and Tsirka, 2011), suggesting that the C-terminus of mouse MCP1 prevents the activation of ERM proteins induced by mouse MCP1. Here we showed that in the presence of A2AP, h-MCP1 dramatically enhanced the intensity of p-ERM, whereas hc-MCP1 did not change the intensity of p-ERM bands at various time points (Figure 4D). Our data suggest that the C-terminus of mouse MCP1 is inhibitory to human MCP1-induced activation of ERM proteins.

Discussion

Although conserved in the N-terminus, the C-terminus of MCP1 varies a lot between species. Compared with human MCP1, rodent MCP1 has a C-terminal tail, which is highly glycosylated (Ernst et al., 1994). In this report we find that appending the mouse C-terminus to the human MCP1 protein results in a decrease of the chemotactic potency of human MCP1 and an attenuation of all the signaling events and cellular changes that accompany the chemotactic stimulation. Moreover we find that the ability of the chimeric chemokine to compromise the BBB is decreased as well.

It is puzzling why the human MCP1 lacks this highly glycosylated C-terminus Search of the databases reveals that only the mouse and rat MCP1 carry this C-terminal extension. One possibility is that the function that the rodent MCP1 C-terminus exerts is no longer needed in human system. It has been shown that the mouse MCP1 C-terminus promotes the oligomerization of the chemokine and thus formation of chemoattractant gradient (Hoogewerf et al., 1997, Lau et al., 2004, Wang et al., 2005, Yao and Tsirka, 2010). Mouse MCP1 without the C-terminus, however, is unable to oligomerize (Yao and Tsirka, 2010). Human MCP1, on the other hand, has been demonstrated to form homodimers in physiological concentrations (Zhang and Rollins, 1995). This finding that human MCP1 does not need a C-terminal fragment to form oligomers may be the reason of the absence of this fragment in human MCP1.

Previous studies in our lab have shown that plasmin cleaves the C-terminal extension off mouse MCP1 in the proximity of the MCP1-generating neurons, generating a fragment highly homologous to human MCP1. This cleaved protein, lacking the C-terminus, has increased chemotactic potency towards microglia (Yao and Tsirka, 2010), and enhances MCP1-induced BBB disruption (Yao and Tsirka, 2011), suggesting that MCP1 activities are

finely regulated by plasmin-mediated truncation in mouse system. Since the human MCP1 lacks the C-terminus, it is unclear whether regulation of human MCP1 is necessary, or whether another protein or protein complex may be responsible for such regulation of human MCP1 activities.

Studies on the MCP1 receptor, CCR2, reveal that only one isoform of CCR2 is found in rodent, but two alternatively spiced isoforms exist in human. The two isoforms of human CCR2, CCR2A and CCR2B, have different C-terminal tails (Charo et al., 1994), suggesting that they may activate different intracellular signaling pathways and thus have different functions, although the molecular cascades downstream of CCR2A and CCR2B are still elusive. So it is conceivable that the regulation of the human MCP1 chemotactic potency is mediated by the CCR2 receptor, rather than the chemokine.

It is not uncommon for chemotactic ligands and receptors to exist in different isoforms: two alternatively spliced variants of EphA7 receptor have different C-termini and show distinct activities in the regulation of cell adhesion (Holmberg et al., 2000). Splicing variants of Robo3, which are different in the C-terminus, have also been reported to exert distinct functions (Chen et al., 2008). Therefore it is likely that the regulation of MCP1/CCR2 interaction and chemoattraction in humans lies with receptor CCR2 or an as-for-now unknown regulatory factor.

Supplementary Material

Refer to Web version on PubMed Central for supplementary material.

Acknowledgments

We would like to thank Drs M. Frohman and M. Garcia-Diaz as well as the members of the Tsirka lab for advice and helpful discussions. This work was partially supported by a SigmaXi grant-in-aid (to YY) and NIH R0142168 (to SET).

References

Bartoli C, Civatte M, Pellissier JF, Figarella-Branger D. CCR2A and CCR2B, the two isoforms of the monocyte chemoattractant protein-1 receptor are up-regulated and expressed by different cell subsets in idiopathic inflammatory myopathies. Acta Neuropathol. 2001; 102:385–392. [PubMed: 11603815]

Biber K, Zuurman MW, Homan H, Boddeke HWGM. Expression of L-CCR in HEK 293 cells reveals functional responses to CCL2, CCL5, CCL7, and CCL8. J Leukocyte Biol. 2003; 74:243–251. [PubMed: 12885941]

Calabria AR, Weidenfeller C, Jones AR, de Vries HE, Shusta EV. Puromycin-purified rat brain microvascular endothelial cell cultures exhibit improved barrier properties in response to glucocorticoid induction. J Neurochem. 2006; 97:922–933. [PubMed: 16573646]

Charo IF, Myers SJ, Herman A, Franci C, Connolly AJ, Coughlin SR. Molecular cloning and functional expression of two monocyte chemoattractant protein 1 receptors reveals alternative splicing of the carboxyl-terminal tails. Proc Natl Acad Sci U S A. 1994; 91:2752–2756. [PubMed: 8146186]

Chen Z, Gore BB, Long H, Ma L, Tessier-Lavigne M. Alternative splicing of the Robo3 axon guidance receptor governs the midline switch from attraction to repulsion. Neuron. 2008; 58:325–332. [PubMed: 18466743]

Deli MA, Abraham CS, Niwa M, Falus A. N,N-diethyl-2-[4-(phenylmethyl)phenoxy]ethanamine increases the permeability of primary mouse cerebral endothelial cell monolayers. Inflamm Res. 2003; 52(Suppl 1):S39–40. [PubMed: 12755402]

Dimitrijevic OB, Stamatovic SM, Keep RF, Andjelkovic AV. Effects of the chemokine CCL2 on blood-brain barrier permeability during ischemia-reperfusion injury. J Cereb Blood Flow Metab. 2006; 26:797–810. [PubMed: 16192992]

Ernst CA, Zhang YJ, Hancock PR, Rutledge BJ, Corless CL, Rollins BJ. Biochemical and biologic characterization of murine monocyte chemoattractant protein-1. Identification of two functional domains. J Immunol. 1994; 152:3541–3549. [PubMed: 8144933]

Giulian D, Baker TJ. Characterization of ameboid microglia isolated from developing mammalian brain. J Neurosci. 1986; 6:2163–2178. [PubMed: 3018187]

Haedicke J, Brown C, Naghavi MH. The brain-specific factor FEZ1 is a determinant of neuronal susceptibility to HIV-1 infection. Proc Natl Acad Sci USA. 2009; 106:14040–5. [PubMed: 19667186]

Holmberg J, Clarke DL, Frisen J. Regulation of repulsion versus adhesion by different splice forms of an Eph receptor. Nature. 2000; 408:203–206. [PubMed: 11089974]

Hoogewerf AJ, Kuschert GS, Proudfoot AE, Borlat F, Clark-Lewis I, Power CA, Wells TN. Glycosaminoglycans mediate cell surface oligomerization of chemokines. Biochemistry. 1997; 36:13570–13578. [PubMed: 9354625]

Lau EK, Paavola CD, Johnson Z, Gaudry JP, Geretti E, Borlat F, Kungl AJ, Proudfoot AE, Handel TM. Identification of the glycosaminoglycan binding site of the CC chemokine, MCP-1: implications for structure and function in vivo. J Biol Chem. 2004; 279:22294–22305. [PubMed: 15033992]

Maghazachi AA. Intracellular signaling events at the leading edge of migrating cells. Int J Biochem Cell Biol. 2000; 32:931–943. [PubMed: 11084373]

Pankov R, Endo Y, Even-Ram S, Araki M, Clark K, Cukierman E, Matsumoto K, Yamada KM. A Rac switch regulates random versus directionally persistent cell migration. J Cell Biol. 2005; 170:793–802. [PubMed: 16129786]

Sheehan JJ, Zhou C, Gravanis I, Rogove AD, Wu YP, Bogenhagen DF, Tsirka SE. Proteolytic activation of monocyte chemoattractant protein-1 by plasmin underlies excitotoxic neurodegeneration in mice. J Neurosci. 2007; 27:1738–1745. [PubMed: 17301181]

Stamatovic SM, Dimitrijevic OB, Keep RF, Andjelkovic AV. Protein kinase Calpha-RhoA cross-talk in CCL2-induced alterations in brain endothelial permeability. J Biol Chem. 2006; 281:8379–8388. [PubMed: 16439355]

Stamatovic SM, Keep RF, Kunkel SL, Andjelkovic AV. Potential role of MCP-1 in endothelial cell tight junction 'opening': signaling via Rho and Rho kinase. J Cell Sci. 2003; 116:4615–4628. [PubMed: 14576355]

Stamatovic SM, Shakui P, Keep RF, Moore BB, Kunkel SL, Van Rooijen N, Andjelkovic AV. Monocyte chemoattractant protein-1 regulation of blood-brain barrier permeability. J Cereb Blood Flow Metab. 2005; 25:593–606. [PubMed: 15689955]

Terashima Y, Onai N, Murai M, Enomoto M, Poonpiriya V, Hamada T, Motomura K, Suwa M, Ezaki T, Haga T, Kanegasaki S, Matsushima K. Pivotal function for cytoplasmic protein FROUNT in CCR2-mediated monocyte chemotaxis. Nat Immunol. 2005; 6:827–835. [PubMed: 15995708]

Tsukamoto T, Nigam S. Tight junction proteins form large complexes and associate with the cytoskeleton in an ATP depletion model for reversible junction assembly. J Biol Chem. 1997; 272:16133–16139. [PubMed: 9195909]

Tsukamoto T, Nigam S. Role of tyrosine phosphorylation in the reassembly of occludin and other tight junction proteins. Am J Physiol. 1999; 276:F737–F750. [PubMed: 10330056]

Wang L, Fuster M, Sriramarao P, Esko JD. Endothelial heparan sulfate deficiency impairs L-selectin- and chemokine-mediated neutrophil trafficking during inflammatory responses. Nat Immunol. 2005; 6:902–910. [PubMed: 16056228]

Yao Y, Tsirka SE. The C terminus of mouse monocyte chemoattractant protein 1 (MCP1) mediates MCP1 dimerization while blocking its chemotactic potency. J Biol Chem. 2010; 285:31509–31516. [PubMed: 20682771]

Yao Y, Tsirka SE. Truncation of Monocyte Chemoattractant Protein-1 by Plasmin Promotes Blood-Brain Barrier Disruption. J Cell Sci. 2011 in press.

Zhang Y, Rollins BJ. A dominant negative inhibitor indicates that monocyte chemoattractant protein 1 functions as a dimer. Mol Cell Biol. 1995; 15:4851–4855. [PubMed: 7651403]

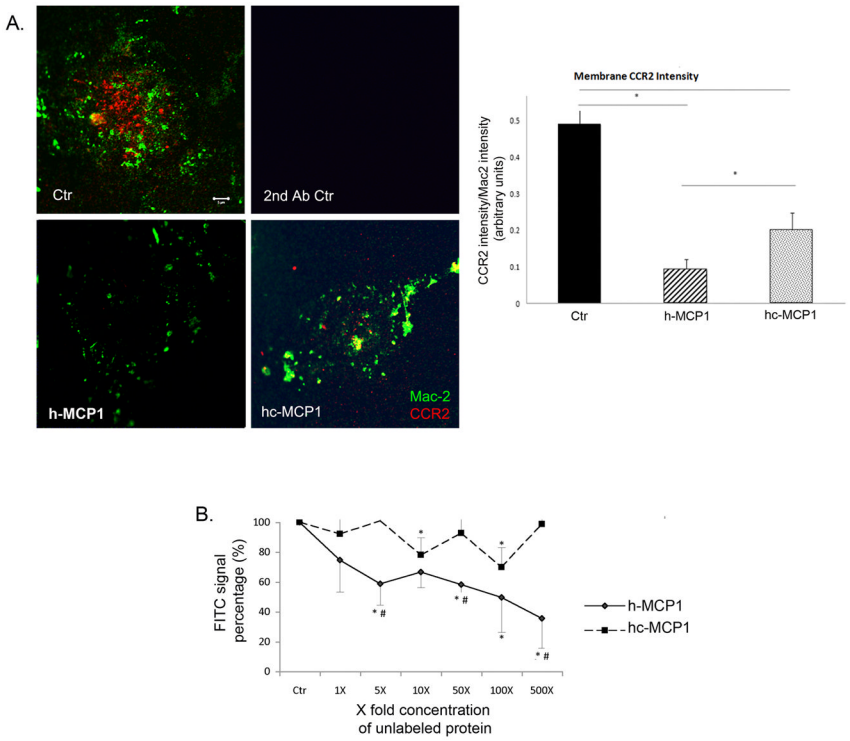

Figure 1. Mouse MCP1 C-terminus decreases the affinity of human MCP1 to CCR2

A. h-MCP1 decreased membrane-bound CCR2 on microglia. Primary microglia activated overnight with 100ng/ml LPS were treated with saline (Ctr) or 10nM recombinant hMCP1 or hc-MCP1 for 1 h and then swelled in hypotonic buffer for 20 min to cause cell lysis. The plasma membrane sheets that adhered to the coverslips were stained for Mac-2 (Green) to visualize the membrane sheets and CCR2 (Red). Microglia immunostained with secondary antibodies only showed no fluorescence. Scale bar = 5 μm. The fluorescent intensity was quantified using ImageJ program and the fluorescent intensity was normalized to plasma membrane area. 20 cells per condition were used and 3 separate experiments were performed. The results were analyzed using student's t-test. *p<0.05. **B.** h-MCP1 has higher affinity for CCR2. Microglia cells (CHME3) were incubated with 50nM biotinylated human MCP1 in the presence or absence of a gradient concentration of unlabeled h- or hc-MCP1 for 1 hour at 4°C. After further incubation with FITC-Avidin for 30 minutes at 4°C, the cells were washed and FITC signal was quantified using a plate reader. Background signal was measured using biotinylated soybean trypsin inhibitor (supplied by R&D) and subtracted from the experimental raw data. Then the FITC signal was normalized to total protein concentration. The final data were expressed as percentage of fluorescence in the absence of unlabeled MCP1. The data were expressed as Mean ± SD (n=4). *p<0.05, compared with Ctr; #p<0.05, comparison between h-MCP1 and hc-MCP1.

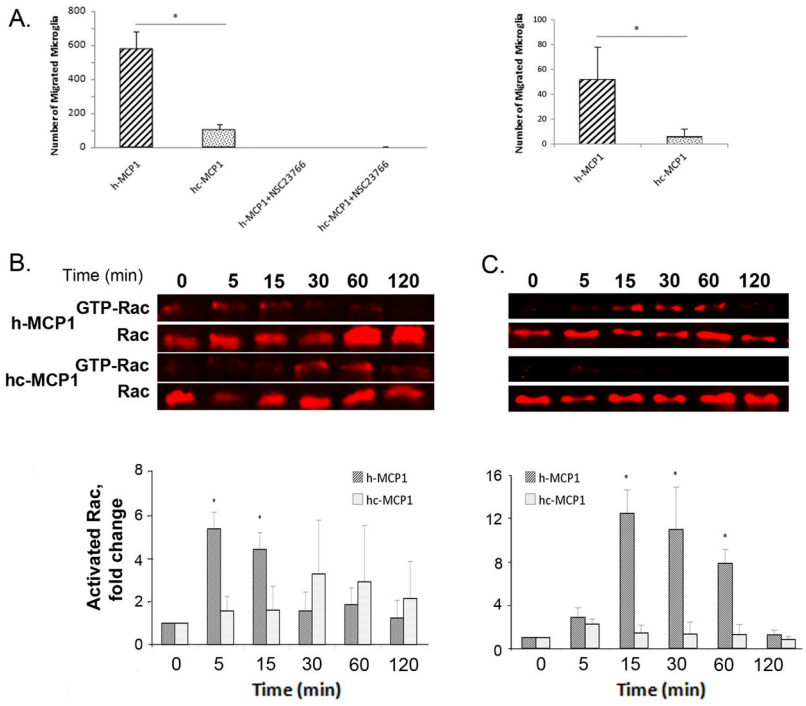

Figure 2. Mouse MCP1 C-terminal extension decreases the chemotactic potency of human MCP1 and the chemotactic activity depends on Rac1

A. Primary mouse microglia (left) or the CHME3 human microglial line (right) were plated and evaluated for chemotaxis in response to recombinant hMCP1 or hc-MCP1, in the presence or absence of the Rac1 inhibitor NSC23766. Each experimental condition was assayed in triplicate. Data are expressed as Mean ± SD. **, $p<0.01$. **B.** N9 microglial cells or **C.** CHME3 human microglial cells were treated with 10nM MCP1 over time. The activated Rac1 was immunoprecipitated using GST-PBD beads. At each time point, the activated and total Rac1 were detected by western blotting. Western blots of activated and total Rac1 and quantification of the blots for hMCP1 and hc-MCP1. The blots were normalized to the 0 time point. Each experimental condition was assayed in triplicate and the data were expressed as Mean ± SD. *$p<0.05$, **$p<0.01$, compared to 0 time point.

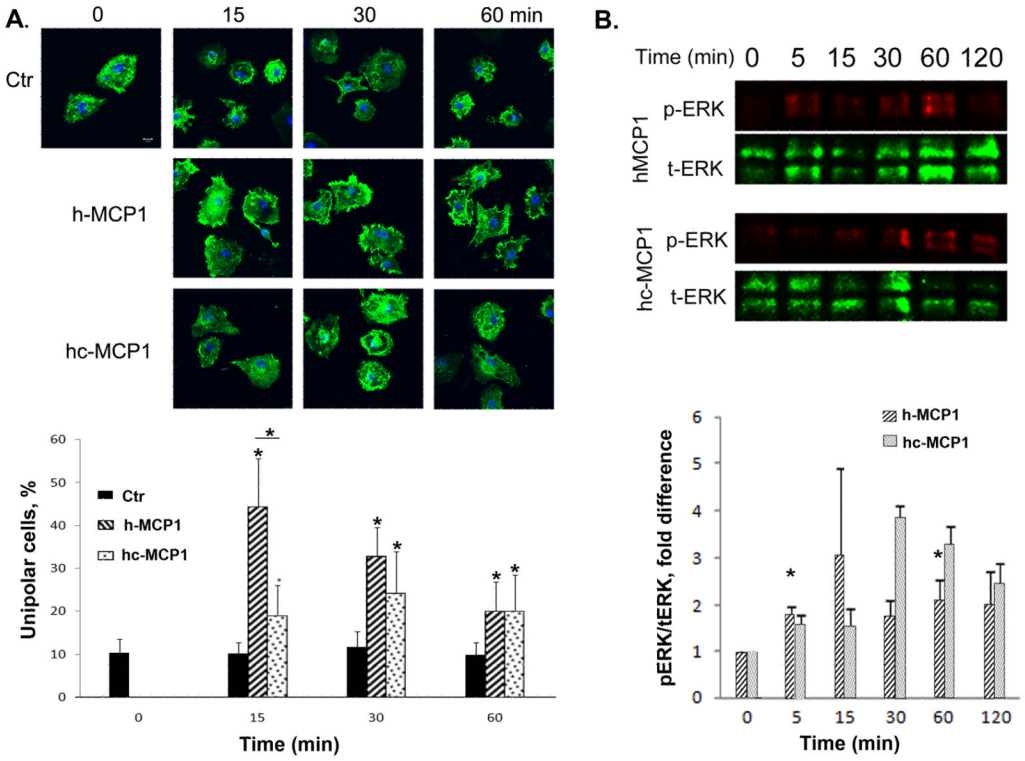

Figure 3. Mouse MCP1 C-terminus inhibits the formation of lamellipodia induced by human MCP1

A. Primary microglia plated on coverslips were incubated with a point source of recombinant MCP1 proteins for different periods of time. At each time point, the cells were washed, fixed, and stained for actin cytoskeleton using Alexa-Phalloidin. Scare bar = 10 μm. The percentage of unipolar cells (migrating towards the focal point of MCP1 protein) was quantified. Data are expressed as Mean ± SD. N=9. *p<0.05. **B.** Mouse MCP1 C-terminus changes the activation pattern of ERK on microglia. Primary microglial cells were treated with h-or hc-MCP1 over time. At each time point, cell lysates were collected and analyzed for phosphorylated and total ERK1/2 by western blotting. Experiments were performed in triplicate. Representative experiment shown. Data are expressed as Mean ± SD. *p<0.05, compared to 0 time point.

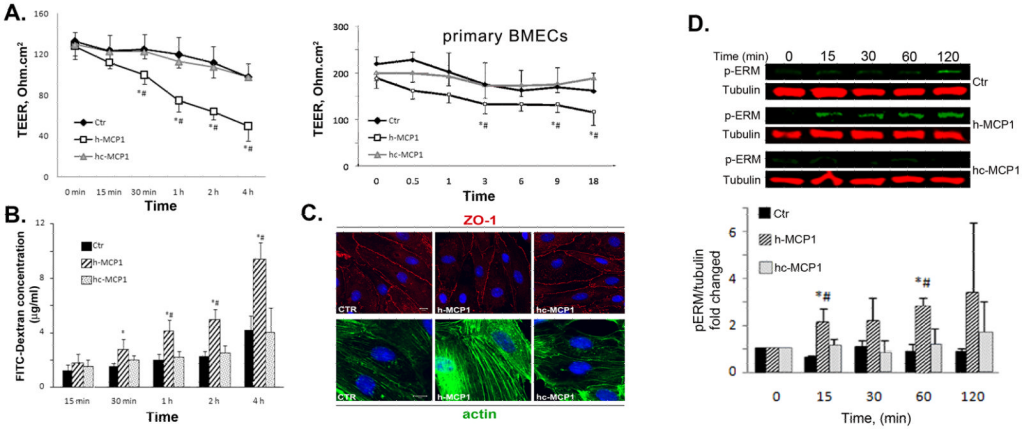

Figure 4. Mouse MCP1 C-terminus inhibits human MCP1-induced BBB compromise

A. Left panel: 100 nM h- or hc-MCP1 was added to the lower chamber of the bEND.3-Astrocyte co-culture system. **Right panel:** Primary BMEC monolayer was treated with 100 nM h- or hc-MCP1 (Primary BMECs). TEER values were determined over time in the presence of A2AP. Values are mean ± SD (n=3–4). TEER values were determined over time in the presence of A2AP. Values are mean ± SD (n=4). **B.** Cells were treated as in **A**. The leakage of FITC-Dextran across the in vitro BBB was determined by a fluorescence plate reader in the presence of A2AP. The concentration of FITC-Dextran in the lower chamber was calculated based on a standard curve. Values are mean ± SD (n=4). Analysis was performed using student's t-test. Comparison with Ctr, *p<0.05 and comparison with hc-MCP1, #p<0.05. **C.** Mouse MCP1 C-terminus inhibits human MCP1-induced redistribution of tight junction proteins. Primary BMEC were treated with 100 nM h- or hc-MCP1 for 2 hours in the presence of A2AP. The cells were then fixed and immunostained for ZO-1 (upper panels) and F-actin (lower panels). **D.** Mouse MCP1 C-terminus is inhibitory to human MCP1-induced phosphorylation of ERM proteins. bEND.3 cells were treated with saline or 100nM h- or hc-MCP1 proteins in the presence of A2AP over time. The phosphorylated ERM proteins were determined using anti-phosphor-ERM antibody. Quantitative data of western blots are shown as mean ± SD (n=3). Comparison with control, *p<0.05 and comparison with hc-MCP1, #p<0.05.